Original Paper

Cellular Physiology and Biochemistry

Cell Physiol Biochem 2012;29:511-522

Accepted: January 11, 2012

Procaterol-stimulated Increases in Ciliary Bend Amplitude and Ciliary Beat Frequency in Mouse Bronchioles

Nobuyo Komatani-Tamiya[a,d,e], Eriko Daikoku[a,b], Yoshizumi Takemura[a,d,e], Chikao Shimamoto[a,f], Takashi Nakano[a,c], Yoshinobu Iwasaki[a,e], Yuka Kohda[a,f], Hitoshi Matsumura[a,f], Yoshinori Marunaka[a,d] and Takashi Nakahari[a,b]

[a]Nakahari Project of Central Research Laboratory, [b]Department of Physiology, and [c]Department of Microbiology and Infection Control, Osaka Medical College, Takatsuki, [d]Department of Molecular Cell Physiology, and [e]Department of Respiratory Medicine, Graduate School of Medical Science, Kyoto Prefectural University of Medicine, Kyoto, and [f]Laboratory of Pharmacotherapy, Osaka University of Pharmaceutical Sciences, Takatsuki

Key Words

Motile cilia • Ciliaed cell • β_2-Adrenergic agonist • cAMP • Mucociliary clearance • Airway

Abstract

The beating cilia play a key role in lung mucociliary transport. The ciliary beating frequency (CBF) and ciliary bend amplitude (CBA) of isolated mouse bronchiolar ciliary cells were measured using a light microscope equipped with a high-speed camera (500 Hz). Procaterol (a β_2-agonist) increased CBA and CBF in a dose dependent manner via cAMP. The time course of CBA increase is distinct from that of CBF increase: procaterol at 10 nM first increased CBA and then CBF. Moreover, 10 pM procaterol increased CBA, not CBF, whereas 10 nM procaterol increased both CBA and CBF. Concentration-response studies of procaterol demonstrated that the CBA curve was shifted to a lower concentration than the CBF curve, which suggests that CBA regulation is different from CBF regulation. Measurements of microbead movements on the bronchiole of lung slices revealed that 10 pM procaterol increased the rate of ciliary transport by 37% and 10 nM procaterol increased it by 70%. In conclusion, we have shown that increased CBA is of particular importance for increasing the bronchiolar ciliary transport rate, although CBF also plays a role in increasing it.

Introduction

The mucociliary transport of the airways, which consists of a surface mucous layer and beating cilia, is a host defence mechanism of the lung. The surface mucous layer traps foreign particles, chemicals, and cellular debris, and the beating cilia transport the surface mucous layer toward the pharynx. Thus, the beating cilia are the engine that drives mucociliary transport [1-6]. The ciliary beat frequency (CBF) is known to be a key factor in controlling the mucociliary transport rate [2-8] and has been measured as an index of ciliary activities in many studies [2-6, 8-13]

Cilia are ubiquitous cellular nanomachines that consist of a microtubule cytoskeleton called the "axoneme". Their beating is maintained by the sliding of microtubule doublets driven by molecular motors, the inner arm dyneins and outer arm dyneins, which are functionally distinct. The inner arm dyneins change the waveform,

KARGER

Fax +41 61 306 12 34
E-Mail karger@karger.ch
www.karger.com

1015-8987/12/0294-0511$38.00/0

Accessible online at:
www.karger.com/cpb

T. Nakahari, M.D.
Department of Physiology, Osaka Medical College,
2-7 Daigaku-cho, Takatsuki 569-8686 (Japan)
Tel. 81 726 83 1221 (ext. 2456), Fax 81 726 84 6520
E-Mail takan@art.osaka-med.ac.jp

whereas the outer arm dyneins affect the frequency [4, 6, 14-20]. In the beating axoneme, an increase in the microtubule doublet sliding velocity has two effects: an increase in bend amplitude (CBA) (Fig. 1) and an increase in beat frequency (CBF) [8].

Patients with inner arm dynein defects, whose cilia showed an abnormal waveform with a markedly reduced CBA but a normal CBF, have the symptoms of primary ciliary dyskinesia (PCD) [14, 15]. In transgenic mice that lack the inner arm dynein heavy chain 7 gene (DyHC7), spermatozoa flagella show an abnormal beating waveform and a decreased lateral amplitude but have a normal CBF. *Chlamydomonas* and *Tetrahymena* mutants lacking DyHC7 also show an irregular ciliary waveform pattern, decreased CBA, slower swim speed, but they still have a normal CBF [19, 21, 22]. These observations suggest that CBA is of particular importance for regulating the mucociliary transport rate in airways. However, no CBA measurements have been carried out in the airway, because it is difficult to observe the fine high-frequency movements of the beating cilia in the airways.

The recent development of video-optical equipment has enabled us to observe the fine movement of individual cilia [2, 23-26]. In this study, we measured CBA and CBF in bronchiolar ciliary cells stimulated by the selective β_2-agonist, procaterol, using a light microscope equipped with a high-speed camera. We found increases in the CBA and CBF of bronchiolar ciliary cells during procaterol stimulation. In this study, we examined the effects of procaterol on CBA and the effects of CBA increase on the bronchiolar ciliary transport rate.

Materials and Methods

Solution and Chemicals

The control solution contained 121 mM NaCl, 4.5 mM KCl, 25 mM $NaHCO_3$, 1 mM $MgCl_2$, 1.5 mM $CaCl_2$, 5 mM NaHEPES, 5 mM HEPES and 5 mM glucose. The Ca^{2+}-free solution contained 121 mM NaCl, 4.5 mM KCl, 25 mM $NaHCO_3$, 1 mM $MgCl_2$, 1 mM EGTA, 5 mM NaHEPES, 5 mM HHEPES and 5 mM glucose. For the cell preparation, we used a nominally Ca^{2+}-free solution, which consisted of the control solution without $CaCl_2$. The solution pH was adjusted to 7.4 by adding 1 M HCl. All solutions were aerated with a gas mixture (95% O_2 and 5% CO_2) at 37°C. The procaterol was a generous gift from Otsuka Pharmaceutical Co., Ltd. (Tokyo, Japan). Forskolin (FK), heparin, elastase, and bovine serum albumin (BSA) were from Wako Pure Chemical Industries, Ltd. (Osaka, Japan), PKI amide was from Enzo Life Sciences International Inc. (Plymouth Meeting, PA, USA), and ICI-118,551 (an inhibitor of β_2-receptor) and DNase I were from Sigma Chemical Co. (St Louis, MO, USA). All reagents were dissolved in dimethyl sulfoxide (DMSO) and prepared to their final concentrations immediately before the experiments. The DMSO concentration did not exceed 0.1%, and DMSO at this concentration had no effect on CBF [11-13, 23].

Cell preparations

Female mice (C57BL/6J, 5 weeks of age) were purchased from SLC Inc. (Hamamatsu, Japan), and fed standard pellet food and water *ad libitum*. Lung epithelial cells, including ciliary cells, were isolated from the lungs as previously described [13, 27]. The mice were anaesthetized with intraperitoneal injections of pentobarbital sodium (60-70 mg/kg) and then heparinized (1000 units/kg). The lungs were cleared of blood by perfusion via the pulmonary artery, and the lungs together with the trachea and heart were removed from the mouse en bloc. A nominally Ca^{2+}-free solution (0.5 ml) was instilled into the lung cavity via the tracheal cannula and then removed. This procedure was repeated four times. The fifth instillation was retained in the lung cavity for 5 min, and the lung cavity was then washed five times with the control solution via the tracheal cannula. Finally, the control solution containing elastase (0.2 mg/ml) and DNase I (0.02 mg/ml) was instilled into the lung cavity and the airway epithelium was digested for 35 min at 37°C. Following this incubation, the mediastinal structures (trachea and heart) and extrapulmonary bronchus were removed. The lobes of both lungs were placed in the control solution containing DNase I (0.02 mg/ml) and BSA (3%) and then minced using fine forceps. The minced tissue was gently agitated for 5 min on ice and filtered through a nylon mesh with a pore size of 300 μm square. The cells were washed three times with centrifugation (160 x *g* for 5 min) and then resuspended in the control solution (4°C). With the exception of the PKI amide experiments, cells were used for experiments within 3 h after isolation.

The procedures and protocols for these experiments were performed in accordance with guidelines of the Animal Research Committee of Osaka Medical College and the guiding principles for the care and use of animals in the field of physiological sciences (Physiological Society of Japan).

CBA and CBF measurements

Cells were placed on a coverslip precoated with Cell-Tak (Becton Dickinson Labware, Bedford, MA, USA). Coverslips were set in a microperfusion chamber (30 μl) mounted on an inverted light microscope (T-2000, NIKON, Tokyo, Japan) connected to a high-speed camera (FASTCAM-512PCI, Photron Ltd., Tokyo, Japan). The stage of the microscope was heated to 37ºC, as CBF is temperature-dependent [2]. The chamber was perfused with the control solution (37ºC) at a constant rate (300 μl/min) and aerated with a gas mixture (95% O_2 and 5% CO_2). Ciliary cells were distinguished from other lung epithelial cells, such as alveolar type-I and type-II cells, by their beating cilia (Fig. 2). Ciliary cells accounted for approximately 10-20% of isolated lung cells. For the CBA and CBF measurements, video images were recorded for 2 s at 500 Hz. Before the experiments, the cells were perfused with the control solution for 5 min and then stimulated with various drugs. After the experiments, data analysis was carried out

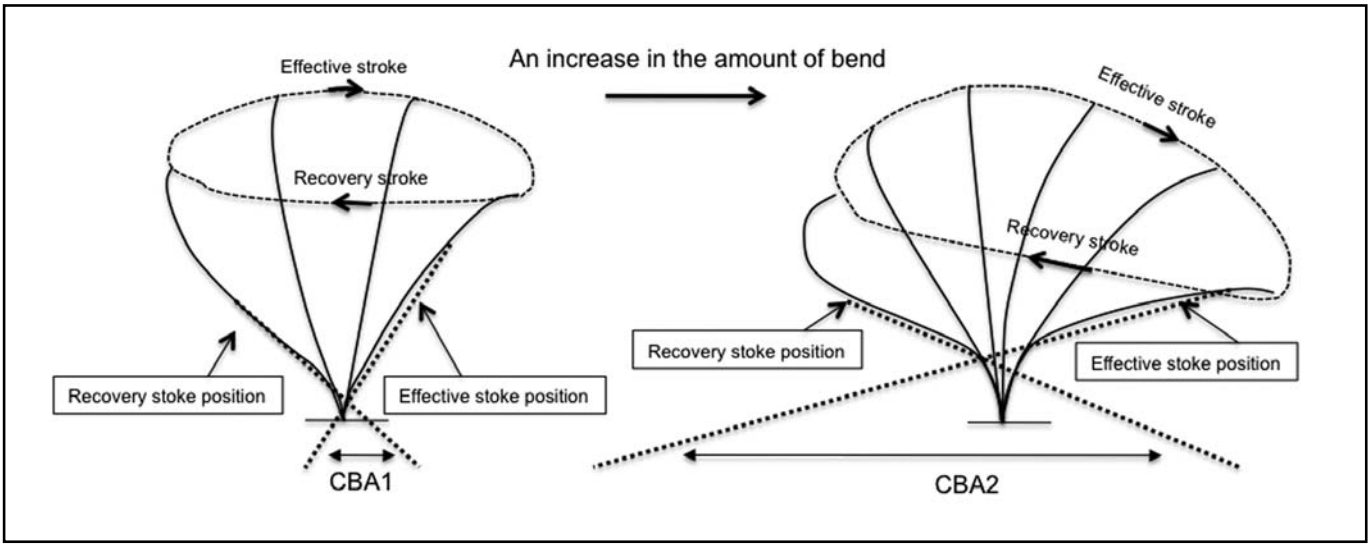

Fig. 1. Schematic diagram of a beating cilium (side view). In the recovery stroke, the cilium starts from the end position of the effective stroke and swings backward close to the cell surface. Then, it fully extends and goes directly through its effective stroke, reaching its maximal velocity in a plane perpendicular to the cell surface [37]. In the effective stroke, the cilium tip makes an arc. The sliding of microtubule doublets in the axoneme forms the bend. To assess the bend, we measured "CBA1" as shown in the right diagram (unstimulated cilium). A stimulus that increases the microtubule doublet sliding velocity in the axoneme increases the magnitude of bend, as shown in the left diagram. To assess the bend, we measured "CBA2", as shown in the left diagram (stimulated cilium).

using an image analysis program (DippMotion 2D, Ditect, Tokyo, Japan).

The CBF measurements are shown in Figs. 2A-C. When we superimposed a line, a-b, on the beating cilia (Fig. 2A) in the video-images, the image analysis program reported changes in the light intensity on the line for 2s. Figures 2B&C show the light intensity changes of the line a-b (Fig. 2A) for 1 s. We could then measure CBF by counting the peaks of these traces. For measurement of CBA, two frame images in a cycle of ciliary beating were selected, one image showing a cilium in the end position of the effective stroke and the other showing the cilium in the start position of the effective stroke. A schematic diagram of CBA change is shown in Fig. 1. White lines were superimposed on the cilium in the final position (Figs. 2D-1 and 2E-1) and in the start position of the effective stroke (Figs. 2D-2 and 2E-2). In Figures 2D-2 and 2E-2, the end positions of the effective stroke (Figs. 2D-1 and 2E-1) were also superimposed. The angle between the two white lines (Fig. 2D-2 or 2E-2) was measured using an image analysis program (DippMotion 2D, Ditect, Tokyo, Japan).

The CBA and CBF ratios (CBA_t/CBA_0 and CBF_t/CBF_0) were used to make comparisons between the experiments. Five CBFs/CBAs measured for 5 min during control perfusion were averaged and the averaged value was used as CBF_0/CBA_0. The subscripts "t" or "0" indicate the time after and before the start of experiments, respectively. Each experiment was carried out using 6-10 cover slips with cells obtained from 3-5 animals. For each coverslip, we selected a visual field with 1-2 cells or cell-blocks as shown in Fig. 2 and measured their CBAs or CBFs. The ratios of CBA and CBF calculated from 4-12 cells were plotted and the cell number was expressed as "n".

Intracellular Ca^{2+} concentration

Intracellular Ca^{2+} concentration was measured using fura 2-acetoxymethyl ester (fura 2-AM). Cells were incubated with 2.5 μM fura 2-AM for 25 min at 23°C and placed in the perfusion chamber. The Fura 2 was excited at 340 and 380 nm and emission at 510 nm was measured using a fluorescence image analysis system (Aqua Cosmos, Hamamatsu Photonics, Hamamatsu, Japan). The fura 2 fluorescence ratios (F340/F380) were calculated. Changes in the intracellular Ca^{2+} concentration were expressed as those in F340/F380. The experiments were carried out using 10 coverslips obtained from 3 animals.

Observation of microbead transport in bronchioles

To assess the rate of ciliary transport in bronchioles, we measured the movement of latex microbeads across the bronchiolar surface in lung slices. Lungs were cut into thin slices using two adherent razor blades (the thickness of a slice was 300-400 μm). The slices were placed on a coverslip precoated with Cell-Tak to allow the slices to adhere firmly. The coverclip with slices was set in the perfusion chamber, which was mounted on a light microscope (BX50WI, Olympus, Tokyo, Japan) connected to a video-enhanced contrast system (Argus 20, Hamamatsu Photonics, Hamamatsu, Japan). The rate of perfusion was 300 μL/min, and the volume of the chamber was 100 μl. The microscope stage was heated to 37°C. The control solution (20 μl, 37°C) containing microbeads (1 μm diameter, 0.2%; polystyrene latex, Nisshin EM Co., Ltd., Tokyo), was added into the chamber. The latex microbeads driven by the beating cilia on the bronchiolar surface were recorded by a video-recorder (30 Hz, National Television System Committie). When microbeads were added into the chamber,

most ran throughout the lung slices with the solution flow in the chamber driven by the perfusion system. However, some microbeads reached bronchiolar surfaces and were transported according to the surface flow driven by ciliary beating (Fig. 9). First, we selected one bronchiole in a lung slice (300-500 μm diameter) and measured the microbead movements across a certain point of the selected bronchiole. In the control experiment, the distance that a microbead was transported for 150 ms (5 frame interval) was measured; the mean distance (d_0) was calculated for 30-90 microbeads. The same measurements and calculations were made for 30-120 microbeads following procaterol stimulation. We also calculated the ratio of microbead movement (d_{stim}/d_0), where the subscripts "stim" and "0" indicate during stimulation and before stimulation, respectively. Each experiment was carried out using 6-10 slices obtained from 3-5 animals.

We also measured the CBA and CBF of the bronchiolar surface in the lung slice. Coverslips with lung slices (the thickness of a slice was 300-400 μm) were placed in a microperfusion chamber (30 μl) mounted on an inverted light microscope (T-2000, NIKON, Tokyo, Japan) connected to a high-speed camera (FASTCAM-512PCI, Photron Ltd., Tokyo, Japan). The microscope stage was heated to 37°C, as CBF depends on temperature [2]. The chamber was perfused with the control solution (37°C) at a constant rate (300 μl/min) and aerated with a gas mixture (95% O_2 and 5% CO_2). We measured CBA and CBF of the bronchiolar surface in the lung slice.

Statistical Analysis

Data are expressed as the mean ± standard error (SEM). Statistical significance between means was assessed by analysis of variance (ANOVA). Differences were considered significant at $p < 0.05$. The statistical analysis results are shown in the figures.

Results

Video images of bronchiolar ciliary cells

The light microscope equipped with a high-speed camera enabled us to observe fine ciliay movements of bronchiolar ciliary cells. Fig. 2A shows six consecutive images taken every 20 ms of bronchiolar ciliary cells isolated from mouse lungs (upper view). During control perfusion, CBF was 10.5 Hz (Fig. 2B). Procaterol stimulation (10 nM) immediately increased the CBF: 5 min after the start of stimulation, the CBF was 23.5 Hz (Fig. 2C).

Procaterol stimulation also increased CBA. Figure 2D and 2E show a ciliary cell (side view) before and 5 min after the addition of 10 nM procaterol (10 nM), respectively. The CBAs before and at 3 min after procaterol stimulation were 92° and 143°, respectively.

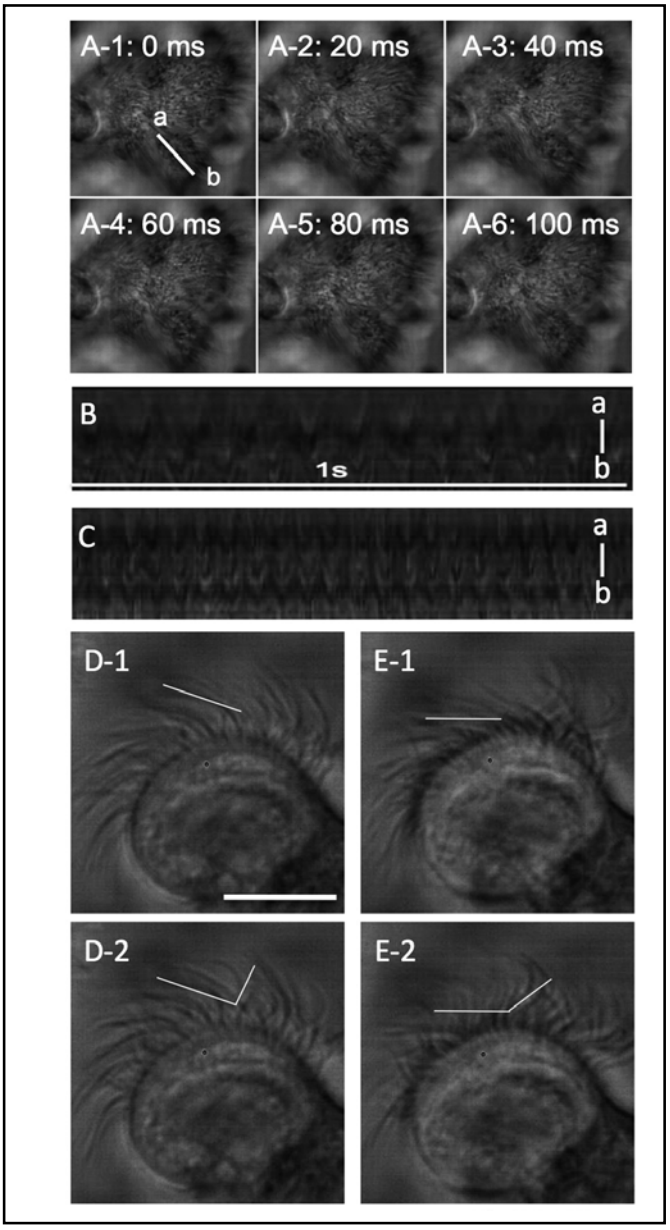

Fig. 2. Video images of ciliary cells isolated from the bronchioles (upper view). A: Six consecutive video images taken every 20 ms. On the apical surface of bronchiolar ciliary cells, the video images clearly show beating cilia. B: Before procaterol stimulation. Changes in light intensity of line a-b marked in panel A1 for 1 s are shown. Ciliary beat frequency (CBF) was measured by counting the peaks. CBF was 11 Hz. C: At 5 min after 10 nM procaterol stimulation, the CBF was increased to 23.5 Hz. D&E: Video-images of bronchiolar ciliary cells (side view). A white line is superimposed on a cilium in the end position of an effective stroke in panels D-1 and panel E-1; a second white line is superimposed on a cilium in the end position of a recovery stroke in panels D-2 and panel E-2. The angle between two lines represents "CBA" (panels D-2 and E-2). D: Before procaterol stimulation. The CBA was 92º. E: During 10 nM procaterol stimulation (3 min after the addition of procaterol), the CBA was 143º. Procaterol (10 nM) significantly increased CBA (panels D-2 and E-2).

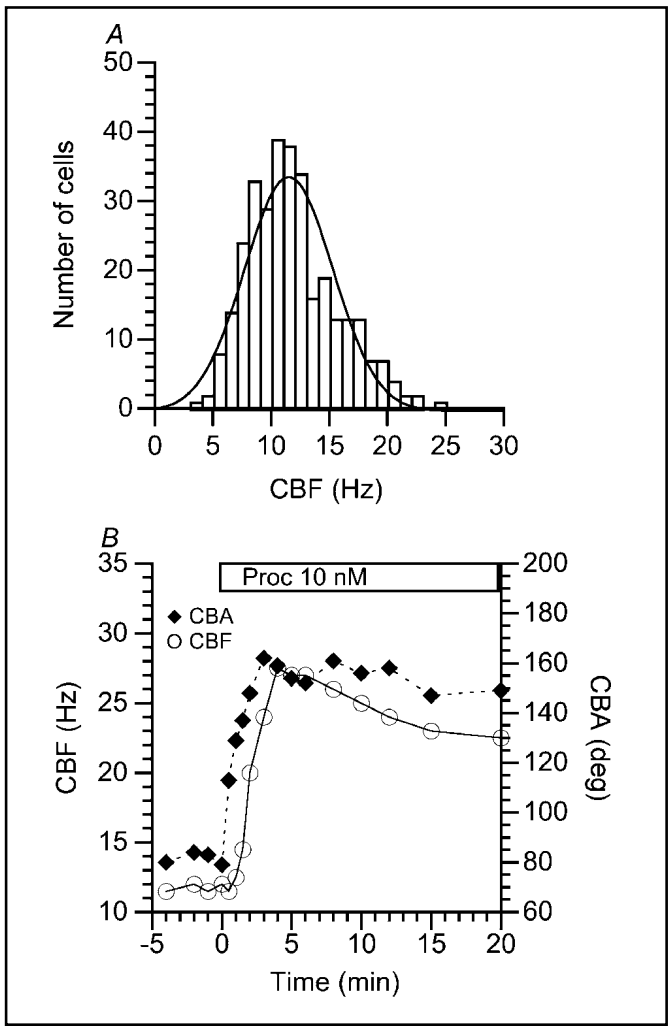

Fig. 3. A: Distribution of ciliary beat frequency (CBF). The columns refer to the number of cells. CBF was measured from ciliary cells isolated from the mouse lungs. A normal distribution curve is superimposed in the same panel. The mean CBF was 11.5 ± 0.2 Hz (n=300). B: Typical changes in CBA and CBF in response to 10 nM procaterol in a bronchiolar ciliary cell. Procaterol stimulation (10 nM) first increased CBA and then increased CBF.

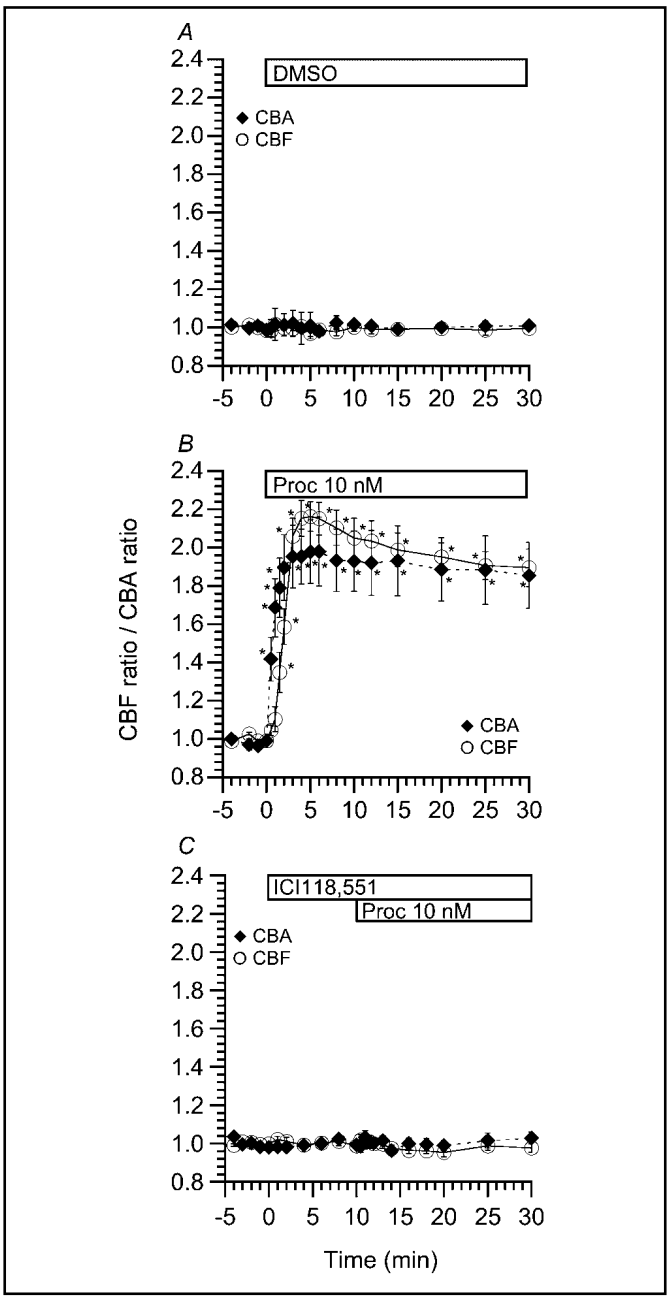

Fig. 4. Effects of ICI-118,551 (a selective β_2-receptor blocker) on CBA and CBF augmented with 10 nM procaterol. The ratios of CBA and CBF were plotted to normalize experiments. A: Control experiments (n=6). DMSO (0.1%) was added to the control solution. B: Stimulation with 10 nM procaterol. *Significantly higher compared with CBA_0 / CBF_0 ($p<0.05$). C: Stimulation with 10 nM procaterol in the presence of ICI-118,551 (10 μM). ICI-118,551 abolished increases in CBA and CBF stimulated by 10 nM procaterol (n=6).

Figure 3A shows the CBF distribution in 300 ciliary cells isolated from mice. The mean CBF without any stimulation was 11.5 ± 0.2 Hz (n=300). The histogram of the CBFs shows a close fit to the normal distribution curve, which is superimposed on the histogram (Fig. 3A). Ciliary cells with CBFs in the range of 9 to 15 Hz were used for experiments.

Effects of procaterol

Figure 3B shows the typical responses in CBA and CBF upon stimulating bronchiolar ciliary cells with 10 nM procaterol. Without any procaterol stimulation, CBA and CBF were constant at baseline (in this case, 80° and 12 Hz). Stimulation with 10 nM procaterol immediately increased CBA, which plateaued within 3 min. The CBAs before and 3 min after stimulation were 79° and 162°,

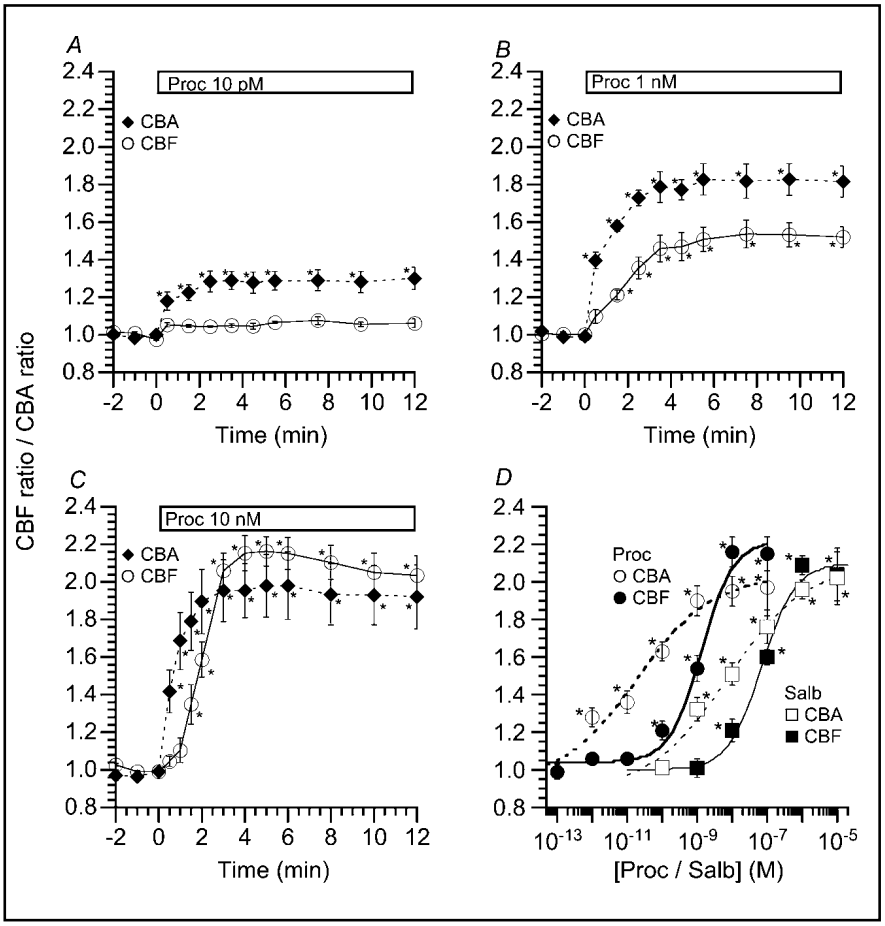

Fig. 5. Effects of procaterol concentration on CBA and CBF in bronchiolarciliary cells. A: Stimulation with 10 pM procaterol increased CBA but not CBF (n=5). *Significantly different ($p<0.05$) from CBA_0. B: Stimulation with 1 nM procaterol. immediately increased CBA and gradually increased CBF, which plateaued within 2.5 min and 3.5 min, respectively. *Significantly different ($p<0.05$) from CBF_0 or CBA_0. C: Stimulation with 10 nM procaterol also immediately increased CBA and gradually increased CBF, which plateaued within 2 min and 3 min, respectively. *Significantly different ($p<0.05$) from CBF_0 or CBA_0. D: Concentration effects of procaterol on CBA and CBF. The ratios of CBA and CBF 5 min after stimulation were plotted against the β_2-agonist concentrations. In the procaterol dose-response study, the curve of CBA ratio was shifted to the left compared with that of CBF ratio (the EC_{50}s of CBA ratio and CBF ratio were 10 pM and 1.1 nM, respectively). Similar results were obtained in the salbutamol concentration-response study (EC_{50}s of CBA ratio and CBF ratio were 7.3 nM and 70 nM, respectively). *Significantly different compared with values obtained using 0.1 pM procaterol or 0.1 nM salbutamol ($p<0.05$).

respectively. Following the CBA increase, the CBF increased from 12 Hz to 27.5 Hz within 4 min and then gradually decreased to 23 Hz by 20 min (Fig. 3B).

To normalize experiments, the ratios of CBA and CBF (CBA_t/CBA_0 and CBF_t/CBF_0) were plotted (Fig. 4). The addition of DMSO (0.1%) had no effect on either CBA or CBF (n=6). Procaterol (10 nM) augmented CBA, which was followed by an increase in CBF. The ratios of CBA/CBF were 1.90 ± 0.17 (n=6)/1.59 ± 0.09 (n=6) at 2 min and 1.95 ± 0.14/2.15 ± 0.09 at 4 min after the procaterol stimulation, respectively. The ratios of CBA/CBF gradually decreased to 1.85 ± 0.17/1.89 ± 0.10 within 30 min (Fig. 4B). The addition of 10 μM ICI-118,551 (a selective β_2-receptor blocker) did not induce any change in the ratios of CBA and CBF (n=8), nor did further stimulation with 10 nM procaterol (Fig. 4C). Changes in CBA and CBF were measured by three blinded observers, who detected similar changes in CBA and CBF.

Next, the concentration effects of procaterol on the ratios of CBA and CBF were examined (Fig. 5). Procaterol at a concentration of less than 0.1 pM did not affect the CBA and CBF ratios (data not shown). Stimulation with 10 pM procaterol caused an increase in the CBA ratio but not in the CBF ratio (Fig. 5A). The ratios of CBA/CBF 4.5 min after procaterol stimulation were 1.28 ± 0.06 (n=6)/1.05 ± 0.01 (n=8). For comparison, the CBA/CBF before and 4.5 min after stimulation were 68°/12 Hz and 84°/12.5 Hz, respectively. Thus, 10 pM procaterol significantly increased the CBA ratio ($p<0.05$), but not the CBF ratio. Stimulation with 1 nM procaterol increased the ratios of CBA/CBF from 1.40 ± 0.04 (n=6)/1.10 ± 0.04 (n=12) at 0.5 min to 1.83 ± 0.08/1.51 ± 0.06 at 5.5 min (Fig. 5B). Stimulation with 10 nM procaterol induced an increase in the CBA ratio followed by an increase in the CBF ratio, as shown in Fig. 4B and 5C. Thus, the ratios of CBA and CBF during stimulation with 1 or 10 nM procaterol increased significantly ($p<0.05$) compared with CBA_0 and CBF_0 (Fig. 5B&C). Figure 5D shows the concentration-response curves of the CBA and CBF ratios. Procaterol increased the ratios of CBA and CBF in a concentration-dependent manner. However, the slope of the CBF curve is steeper than that of the CBA curve. The half-maximum concentrations (EC_{50}) were 20 pM for CBA and 1.3 nM for CBF. Thus, the concentration-response curve of CBA is distinct from that of CBF. These observations suggest that the regulation

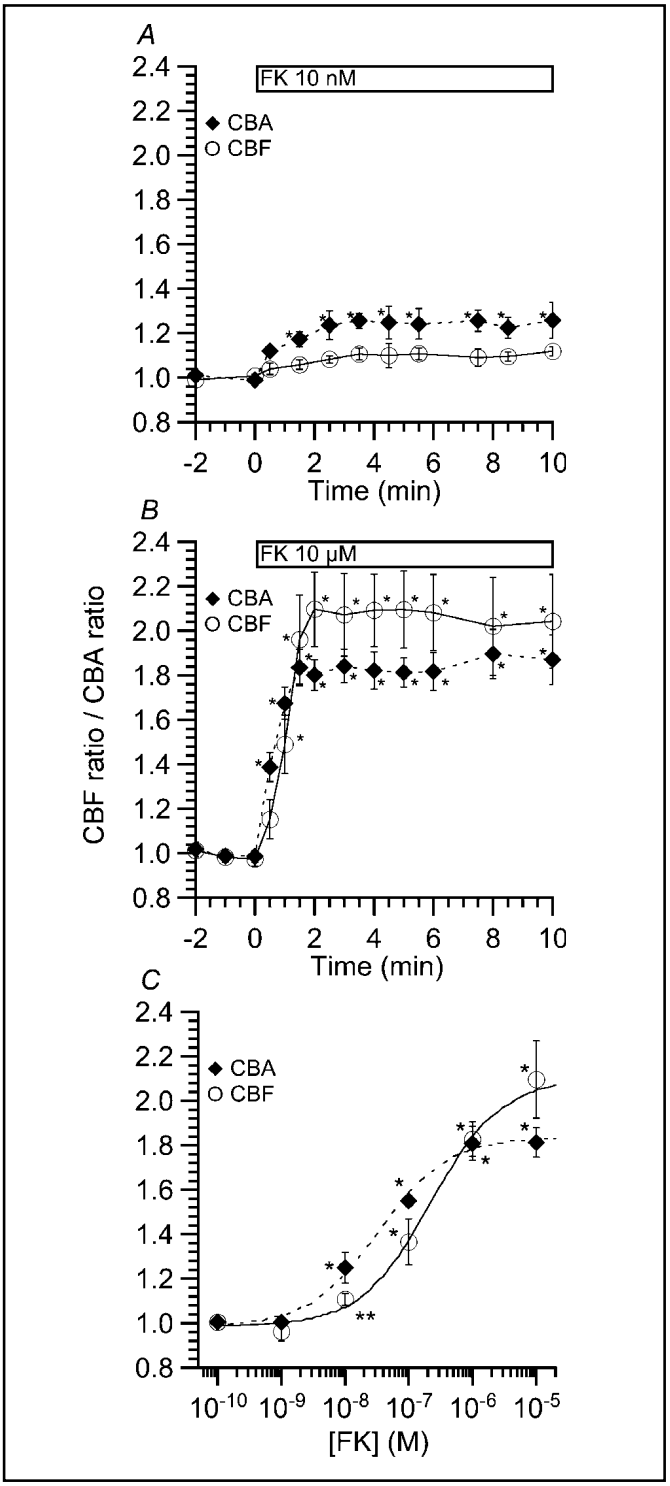

Fig. 6. Effects of FK concentration on CBA and CBF in bronchiolar ciliary cells. A: Stimulation with 10 nM FK significantly increased the CBA ratio, but it increased the CBF ratio only slightly. B: Stimulation with 10 µM FK first increased CBA and then augmented CBF. *Significantly different from values at time 0 (p<0.05). C: Dose-dependent effects of FK on CBA and CBF ratios 5 min after the start of FK stimulation. The dose-response curve of CBA ratio shifted to the left from that of CBF ratio. *Significantly different from values obtained using 1 nM FK (p<0.05).

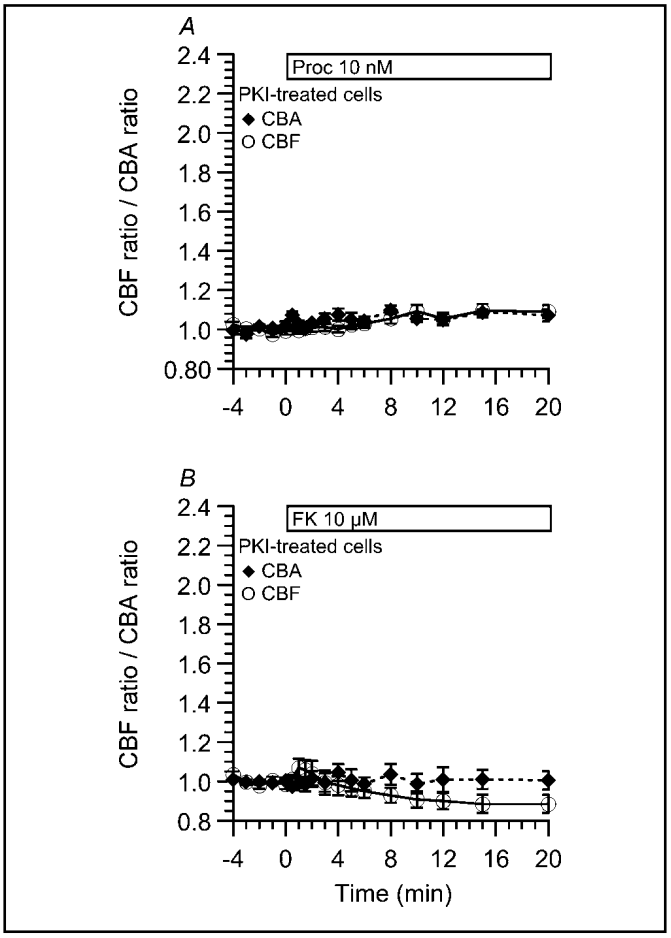

Fig. 7. Effects of PKI amide (a PKA inhibitor) on the ratios of CBA and CBF stimulated by 10 nM procaterol. Cells were treated with 50 µM PKI amide for 3 h prior to stimulation with procaterol (10 nM) or FK (10 µM). PKI amide abolished increases in CBA and CBF stimulated by 10 nM procaterol (A) or 10 µM FK (B).

pathway of the CBA is different from that of CBF and show that procaterol is more effective to CBA than CBF.

The effects of salbutamol (a selective β_2-agonist) on CBF and CBA were also examined. Salbutamol, similarly to procaterol, increased the CBA and CBF ratios in a concentration-dependent manner, and the concentration-response curve of CBA is distinct from that of CBF (Fig. 5D). The EC_{50}s of salbutamol were 7.3 nM for CBA and 70 nM for CBF. Experiments were also carried out using terbutaline (another selective β_2-agonist) and the concentration-response curve of CBA was again distinct from that of CBF. The EC_{50}s of of terbutaline were 66 nM for CBA and 370 nM for CBF (data not shown). Thus, three selective β_2-agonists increased both CBA and CBF and are more effective to CBA than CBF as shown in the distinct EC_{50}s. However, the EC_{50}s of

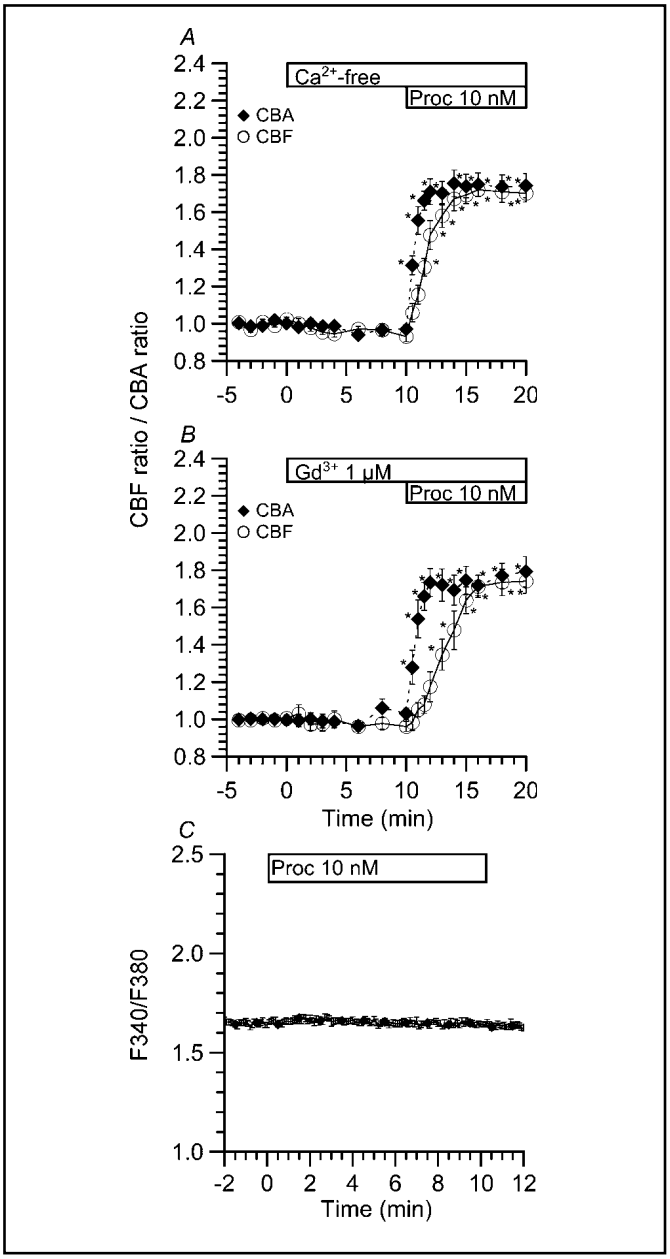

Fig. 8. Effects of Ca^{2+}-free solution and Gd^{3+} on CBA and CBF ratio increases stimulated by 10 nM procaterol. A: Effects of Ca^{2+}-free solution. When cells were perfused with a Ca^{2+}-free solution, no changes in basal CBA and CBF were noted. Stimulation with 10 nM procaterol immediately increased CBA (within 2 min) and then gradually increased CBF (within 5 min). The procaterol-stimulated plateau ratios of CBA and CBF in the absence of Ca^{2+} were 80% of those in the presence of Ca^{2+}. B: Effects of 1 μM Gd^{3+}. The addition of 1 μM Gd^{3+} did not decrease basal CBA and CBF. Stimulation with 10 nM procaterol immediately increased the CBA (within 2 min) and gradually increased the CBF (within 6 min). The final ratios of CBA and CBF in the presence of 1 μM Gd^{3+} were 80% of those in the absence of 1 μM Gd^{3+}. C: Changes in $[Ca^{2+}]_i$. Stimulation with 10 nM procaterol did not induce any increase in the fura 2 fluorescence ratio (F340/F380). *Significantly different from values obtained using 1 nM FK (p<0.05).

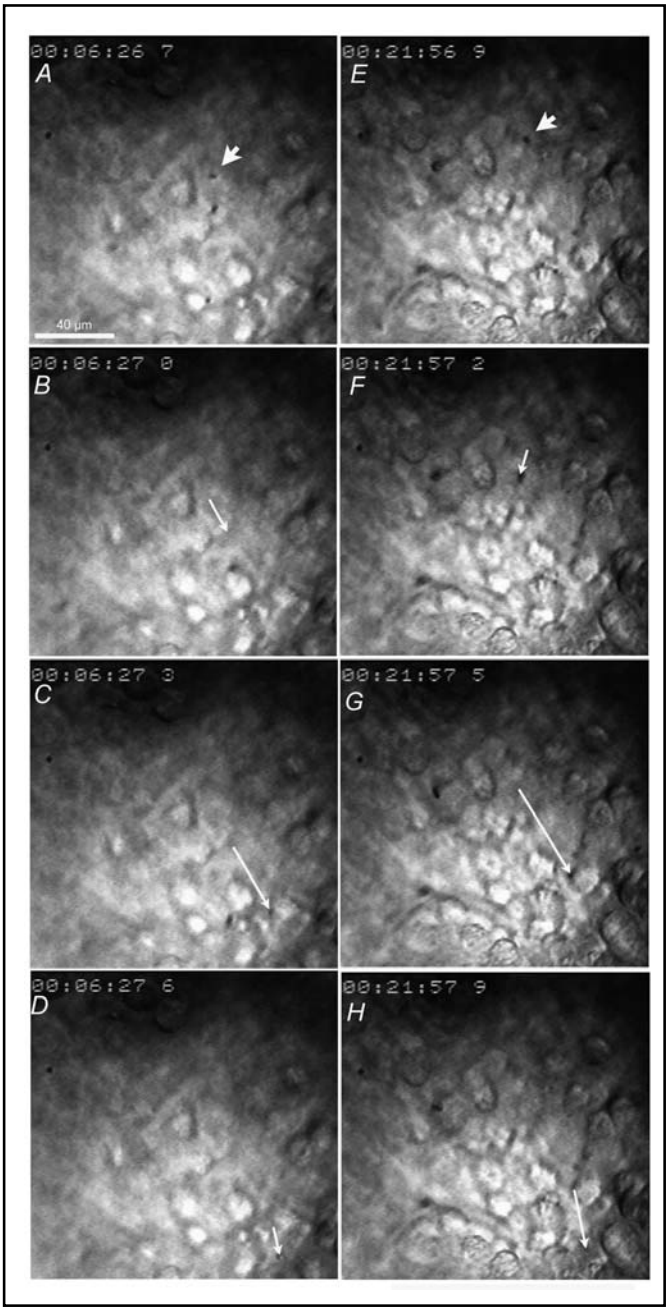

Fig. 9. Movements of a latex microbead on the bronchiolar surface. Panels A-D (before stimulation) and panels E-H (during 1 nM procaterol stimulation) show four consecutive video frame images taken every 300 ms (10 frame interval). The initial position of the bead is marked by arrows (bold face) in panels A and E. White arrows in panels B-D and F-H show the movement of a latex microbead over 300 ms (10 frame interval).

three β_2-agonists were different (procaterol < salbutamol < terbutaline) because of their different chemical structures.

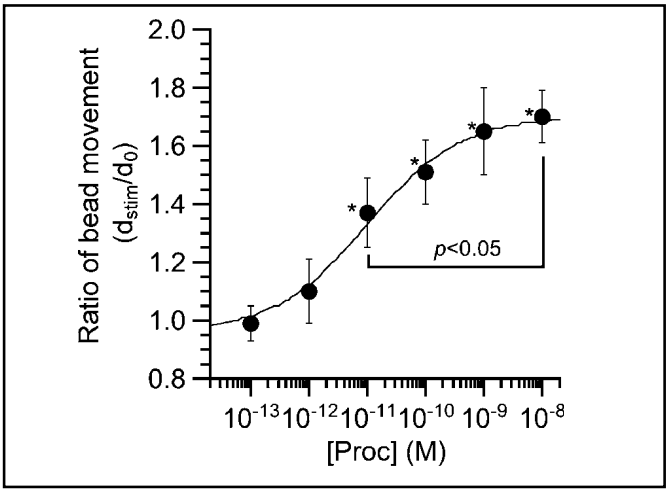

Fig. 10. Effects of procaterol concentration on latex microbead movement in the bronchioles. The distance ratio of microbead movement (d_{stim}/d_0) was calculated from the mean distance of microbead movements (30-120 beads) for 150 - 300 ms before and after stimulation. The results obtained from 4-8 experiments for each procaterol concentration are plotted. Procaterol (10 pM) significantly increased the distance ratio of microbead movement. *Significantly different from values obtained using 0.01 pM procaterol ($p<0.05$). The ratio for 10 nM procaterol is significantly higher than that for 10 pM procaterol ($p<0.05$).

Effects of cAMP accumulation

The effects of cAMP accumulation on the CBA and CBF ratios were examined, because β_2-agonists stimulate cAMP accumulation. Stimulation with 1 nM forskolin (FK) did not increase CBA or CBF (data not shown). Stimulation with 10 nM FK induced increases in CBA but not CBF. The ratios of CBA and CBF 5 min after stimulation were 1.25 ± 0.07 (n=4) and 1.15 ± 0.05 (n=5), respectively (Fig. 6A). Thus, 10 nM FK significantly increased the CBA ratio ($p<0.05$), but not CBF ratio. Stimulation with 10 μM FK induced a CBA increase followed by a CBF increase (Fig. 6B). The ratios of CBA/CBF were 1.39 ± 0.06 (n=4)/1.15 ± 0.09 (n=5) at 0.5 min after stimulation and 1.81 ± 0.07/2.10 ± 0.17 at 5 min after stimulation. For example, CBAs/CBFs in one experiment were 67º/9.5Hz before and 115º/20Hz at 5 min after stimulation. The dose effects of FK on the ratios of CBA and CBF are shown in Fig 6C: the dose-response curve of CBA (EC_{50} = 23 nM) was distinct from that of CBF (EC_{50} = 220 nM). Thus, FK was more effetive to CBA than CBF, similar to procaterol.

We then tested the effects of PKI amide (a PKA inhibitor) on increases in CBA and CBF stimulated by 10 nM procaterol. Cells were treated with PKI amide (50 μM) for 3 h at 23°C and then, set in the perfusion chamber.

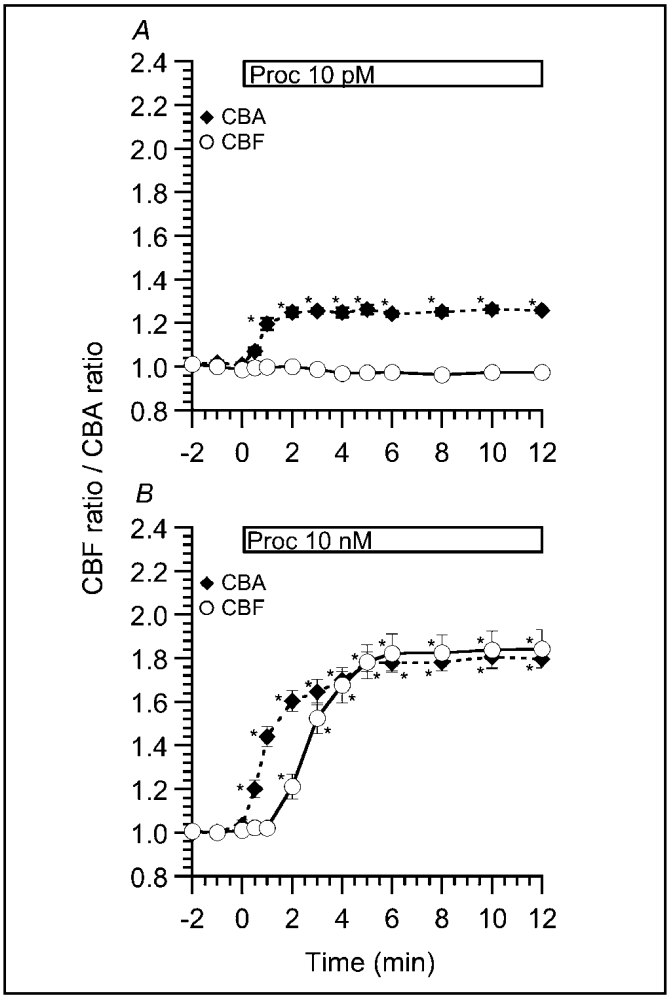

Fig. 11. Changes in CBA and CBF of the bronchiolar surface in lung slices during procaterol stimulation. A: Stimulation with 10 pM procaterol increased CBA but not CBF (n=7). B: Stimulation with 10 nM procaterol also immediately increased CBA and gradually increased CBF. The CBA and CBF plateaued within 2 min and 4 min, respectively. *Significantly different ($p<0.05$) from CBF_0 or CBA_0.

Stimulation with 10 nM procaterol did not increase in CBA or CBF in the presence of PKI amide. The ratios of CBA and CBF 4 min after the addition of procaterol stimulation were 1.08 ± 0.03 (n= 6) and 1.00 ± 0.02 (n=10), respectively. Thus, pretreatment of PKI amide abolished the procaterol-induced increases in the CBA and CBF ratios (Fig. 7A). Treatment with PKI amide also abolished increases in CBA and CBF stimulated by 10 μM FK (Fig. 7B). When we treated cells with PKI amide for 2h, the increases in CBA and CBF in response to 10 nM procaterol were 50-80% of those that occurred in the absence of PKI amide. The membranes of bronchiolar ciliary cells appear to have a low permeability to PKI amide.

Effects of Ca^{2+}

The effects of extracellular Ca^{2+} on procaterol stimulation were also examined. Incubation in a Ca^{2+}-free solution containing 1 mM EGTA did not affect the CBA and CBF ratios, which were 0.97 ± 0.02 (n= 9) and 1.02 ± 0.01 (n=7) 10 min after switching to a Ca^{2+}-free solution, respectively. Stimulation with 10 nM procaterol immediately increased CBA and then gradually increased CBF. The ratios of CBA/CBF were 1.71 ± 0.07 (n= 9)/ 1.47 ± 0.08 (n=7) at 2 min after stimulation and 1.74 ± 0.06/ 1.69 ± 0.05 at 5 min (Fig. 8A). We examined the effects of 1 μM Gd^{3+} (an inhibitor of store-operated Ca^{2+} channels), because the tracheal ciliary cells in primary culture have been reported to have store-operated Ca^{2+} entry pathways (10). The addition of 1 μM Gd^{3+} did not affect CBA or CBF. Stimulation with 10 nM procaterol induced an immediate increase in CBA, and a gradual increase in CBF. The ratios of CBA/CBF were 1.73 ± 0.07 (n= 4)/1.17 ± 0.08 (n=8) at 2 min after stimulation and 1.74 ± 0.08/1.63 ± 0.07 at 5 min (Fig. 8B). Thus, procaterol significantly increased the ratios of CBA and CBF (p<0.05) in a Ca^{2+}-free solution and in the presence of 1 μM Gd^{3+}. However, the final ratios of CBA and CBF were small (80%) and the rates of CBA increase and CBF increase were slow, compared with those in the control solution. Thus, procaterol actions were not mediated via an increase in intracelullar Ca^{2+} concentration, but intracellular Ca^{2+} may play a role during procaterol stimulation, such as the rate of cAMP accumulation and the maintenance of PKA actions.

A typical response in intracellular Ca^{2+} concentration during procaterol stimulation is shown in Fig. 8C: stimulation with 10 nM procaterol did not increase the F340/F380 ratio in bronchiolar ciliary cells.

Latex microbead transport in the bronchiolar surface

A video-microscope enabled us to observe the ciliary beating on the bronchiolar surface of lung slices (Fig. 9). Figure 9 shows two sets of four consecutive microscope images of a bronchiole in a lung slice taken every 300 ms (10 frames interval). The white arrows in panels B-D and F-H show the movement of a latex microbead, which is driven by beating cilia over a periof of 300 ms. Figures 9A-D show the movement of a latex microbead in a bronchiole before stimulation. In Fig. 9A-D, a microbead was transported approximately 100 μm for 1 s. Figures 9E-H show the movement of a latex microbead at 11 min after 1 nM procaterol stimulation. In Fig. 9E-H, a microbead was transported approximately 170 μm for 1 s.

Figure 10 shows the effects of procaterol concentration on the distance ratio of latex microbead movement (d_{stim}/d_0) in the bronchioles of lung slices. The ratios were 1.10 ± 0.11 (n=6) at 1 pM, 1.37 ± 0.12 (n=8) at 10 pM and 1.70 ± 0.09 (n=8) at 10 nM. The ratio at 10 pM is high compared with that of 1 pM (p<0.05) and the ratio at 10 nM is significantly higher than that at 10 pM (p<0.05).

Figure 11 shows the changes in the CBA and CBF ratios of bronchiolar surface in the lung slices. Stimulation with 10 pM procaterol increased CBA, but not CBF (Fig. 11A), whereas stimulation with 10 nM procaterol increased both (Fig. 11B). Thus, the changes in CBA and CBF in lung slices are similar to those in experiments using isolated cells (Fig. 5).

These results indicate that an increase in CBA with no increase in CBF enhanced microbead movement at the bronchiolar surface and that increases in both CBA and CBF further enhanced microbead movement.

Discussion

This study demonstrated that increased CBA is a key factor in increasing the ciliary transport rate on the bronchiolar surface. The sliding verocity of the microtuble doublet genarates the bend of axoneme and its increase elevates CBF, assuming a constant CBA in the beating axoneme. Under the same assumption (constant CBA), Ross and Corrsin (1974) proposed a theoretical model of beating cilia in airways, in which an increase in CBF enhances the rate of mucociliary transport [7]. Based on these findings, CBF was established as a key parameter for controlling the rate of ciliary transport and has been measured in most studies [2, 4, 10-13]. However, an increase in the microtubule doublets sliding velocity also enhances the axoneme bending, indicating that the increased sliding velocity increases CBA. In this study, we found that procaterol stimulation increases CBA mediated via cAMP accumulation in bronchiolar ciliary cells, although it also increases CBF. This is the first report showing a cAMP-mediated increase in CBA in bronchiolar ciliary cells.

This study also demonstrated that, upon stimulating cAMP accumulation, the time course of CBA increase is distinct from that of CBF increase. The difference between the two time courses suggests that the kinetics of CBA regulation are different from that of CBF, and the regulation pathway of CBA is different from that of CBF. The concentration-response studies with procaterol

and FK indicate that the concentration of cAMP necessary to increase CBA is lower than that for CBF.

On the other hand, studies in *Chlamydomonas* and *Tetrahymena* mutants showed that the inner arm dyneins and outer arm dyneins are functionally distinct: the outer arm dyneins control CBF, and the inner arm dyneins control the waveform including CBA [14-18]. One possible explanation is that cAMP concentrations in microdomains for regulating CBA and CBF activities (inner arm dyneins and outer arm dyneins, respectively) may be different, although it remains unknown why the regulations in CBA and CBF activities are different. Further studies are required to clarify the cAMP compartmentalization in the cilium.

The other finding of this study is that an increase in CBA is of particular importance in activating the ciliary transport on the bronchiolar surface; an increase in CBA enhances the rate of ciliary transport on the bronchiolar surface. The patients with primary ciliary dyskinesia (PCD), mice and *Tetrahymena* with inner arm dynein defects have revealed that CBA is of particular importance for maintaining cilia functions. Patients with inner arm dynein defects whose cilia show an abnormal waveform with a stiff forward stroke, markedly reduced CBA, but normal CBF have symptoms of PCD in the lung, nose, sinus, ear, and situs inversus [14, 15]. In the spermatozoa from mice lacking the inner arm dynein heavy chain 7 (DyHC7) gene, the lateral amplitude of the flagella beat is decreased by 50% compared with controls, resulting in reduced swimming velocities of spermatozoa, but their CBF was unaffected [28]. In *Tetrahymena*, DyHC6- or 7-knockout mutants show an irregular ciliary beat waveform, a normal CBF, and decreased swim speeds [19-21]. Thus, the results of this study are consistent with those previously reported in PCD patients, mice and *Tetrahymena* with inner arm dynein defects: that is, that an increase in CBA is the key factor controlling the rate of ciliary transport.

In *Chlamydomonas*, PKA bound to an A-kinase anchoring protein (AKAP) is a structural component of axonemes, which include inner arm dyneins, central pair apparatus, and the radial spokes. An AKAP homologue has been found in axonemes of human and bovine airway cilia [29, 30]. The outer arm dyneins are phosphorylated by PKA in *Tetrahymena* cilia [31, 32]. Thus, PKA controls a signalling pathway involving the central pair apparatus, radial spokes, and inner arm dyneins and outer arm dyneins in *Chlamydomonas* and *Tetrahymena* [33-36]. Similar signalling pathways activated by cAMP may regulate CBA and CBF in the bronchiolar ciliary cells.

We also showed that increasing the CBF enhances the microbead transport rate. The rate of microbead transport stimulated with 10 nM procaterol was higher than that stimulated with 10 pM procaterol (Figs. 5, 10 and 11); stimulation with 10 nM procaterol increased CBA and CBF, whereas 10 pM procaterol only increased CBA. Thus, an increase in CBF facilitates the rate of ciliary transport, as previously reported [7, 8].

In conclusion, this study demonstrates that 1) CBA is of primary importance for increasing the ciliary transport rate, and that 2) CBF plays a secondary role in enhancing the ciliary transport rate, as previously reported [7, 8].

Acknowledgements

Supplemental movies showing the ciliary beating of bronchiolar cells and microbead movements in the bronchioles are shown in the homepage of T. Nakahari (http://www.osaka-med.ac.jp/perso/nakahari/cpb-sup/).We express many thanks to Otsuka Pharmaceutical Co., Ltd. especially, Mr. Shigeru Kobayashi and Miss Yoshiko Abe, for giving an opportunity to do this experiment.

References

1 Afzelius BA: Cilia-related diseases. J Pathol 2004;204:470-477.

2 Delmotte P, Sanderson MJ: Ciliary beat frequency is maintained at maximal rate in the small airways of mouse lung slices. Am J Respir Cell Mol Biol 2006;35:110-117.

3 Knowles MR, Boucher RC: Mucus clearance as a primary innate defense mechanism for mammalian airways. J Clin Invest 2002;109:571-577.

4 Salathe M: Regulation of mammalian ciliary beating. Annu Rev Physiol 2007;69:401-422.

5 Satir P, Christensen ST: Overview of structure and function of mammalian cilia. Annu Rev Physiol 2007;69:377-400.

6 Wanner A, Salathe M, O'riordan TG: Mucociliary clearance in the airways. Am J Respir Crit Care Med 1996;154:1968-1902.

7 Ross SM, Corrsin S: Results of analytical model of mucociliary pumping. J Appl Physiol 1974;37:333-340.

8 Satir P, Barklow K, Hamasaki T: The control of ciliary beat frequency. Trend Cell Biol 1993;3:409-412.

9 Smith RP, Shellard R, Dhillon DP, Winter J, Mehta A: Asymmetric interactions between phosphorylation pathways regulating ciliary beat frequency in human nasal respiratory epithelium in vitro. J Physiol 1996;496:883-889.

10 Lorenzo IM, Liedtke W, Sanderson MJ, Valverde MA: TRPV4 channel participates in receptor-operated calcium entry and ciliary beat frequency regulation in mouse airway epithelial cells. Proc Natl Acad Sci USA 2008;105:12611-12616.
11 Hayashi T, Kawakami M, Sasaki S, Katsumata T, Mori H, Yoshida H, Nakahari T: ATP regulation of ciliary beat frequency in rat tracheal and distal airway epithelium. Exp Physiol 2005;90:535-544.
12 Kawakami M, Nagira T, Hayashi T, Shimamoto C, Kubota T, Mori H, Yoshida H, Nakahari T: Hypo-osmotic potentiation of acetylcholine-stimulated ciliary beat frequency through ATP release in rat tracheal ciliary cells. Exp Physiol 2004;89:739-751.
13 Shiima-Kinoshita C, Min K-Y, Hanafusa T, Mori H, Nakahari T: β2-adrenergic regulation of ciliary beat frequency in rat bronchiolar epithelium: potentiation by isosmotic cell shrinkage. J Physiol 2004;554:403-416
14 Chilvers MA, Rutman A, O'Callaghan C: Ciliary beat pattern is associated with specific ultrastructural defects in primary ciliary dyskinesia. J Allergy Clin Immunol 2003;112:518-524.
15 De Iongh RU, Rutland J: Ciliary defects in healthy subjects, bronchiectasis, and primary ciliary dyskinesia. Am J Respir Crit Care Med 1995;151:1559-1567.
16 Brokaw CJ: Control of flagellar bending: a new agenda based on dynein diversity. Cell Motil Cytoskeleton 1994;28:199-204.
17 Brokaw CJ, Kamiya R: Bending patterns of *Chlamydomonas* flagella: IV. Mutants with defects in inner and outer dynein arms indicate differences in dynein arm function. Cell Motil Cytoskeleton 1987;8:68-75.
18 Hard R, Blaustein K, Scarcello L: Reactivation of outer arm-depleted lung axonemes: evidence for functional differences between inner and outer dynein arms in situ. Cell Motil Cytoskeleton 1992;21:199-209.
19 Wood CR, Hard R, Hennessey TM: Targeted gene disruption of dynein heavy chain 7 of *Tetrahymena thermophila* results in altered ciliary waveform and reduced swim speed. J Cell Sci 2007;120:3075-3085.
20 Movassagh T, Bui KH, Sakakibara H, Oiwa K, Ishikawa T: Nucleotide-induced global conformational changes of flagellar dynein arms revealed by insitu analysis. Nat Struct Mol Biol 2010;17:761-767.
21 Angus SP, Edelmann RE, Pennock DG: Targeted gene knockout of inner arm 1 in *Tetrahymena thermophila*. Eur J Cell Biol 2001;80:486-497.
22 Hennessey TM, Kim DY, Oberski DJ, Hard R, Rankin SA, Pennock DG: Inner arm dynein 1 is essential for Ca^{++}-dependent ciliary reversals in *Tetrahymena thermophila*. Cell Motil Cytoskeleton 2002;53:281-288.
23 Matsubara E, Nakahari T, Yoshida H, Kuroiwa T, Harada K, Inoue K, Koizumi A: Effects of perfluorooctane sulfonate on tracheal ciliary beating frequency in mice. Toxicol 2007;236:190-198.
24 Suzuki T, Miyamoto H, Nakahari T, Inoue I, Suemoto T, Jiang B, Hirota Y, Itohara S, Saido TC, Tsumot T, Sawamoto K, Hensch TK, Delgado-Escueta AV, Yamakawa K: Efhc1 deficiency causes spontaneous myoclonus and increased seizure susceptibility. Hum Mol Genet 2009;18:1099-1109.
25 Takaki E, Fujimoto M, Nakahari T, Yonemura S, Miyata Y, Hayashida N, Yamamoto K, Vallee RB, Mikuriya T, Sugahara K, Yamashita H, Inouye S, Nakai A: Heat shock transcription factor 1 is required for maintenance of ciliary beating in mice. J Biol Chem 2007;282:37285-37292.
26 Nishimura A, Sakuma K, Shimamoto C, Ito S, Nakano T, Daikoku E, Ohmichi M, Ushiroyama T, Ueki M, Kuwabara H, Mori H, Nakahari T: Ciliary beat frequency controlled by oestradiol and progesterone during ovarian cycle in guinea-pig Fallopian tube. Exp Physiol 2010;95:819-828.
27 Tokuda S, Chimamoto C, Yoshida H, Murao H, Kishima G, Ito S, Kubota T, Hanafusa T, Sugimoto T, Niisato N, Marunaka Y, Nakahari T: HCO_3^--dependent pH_i recovery and overacidification induced by NH_4^+ pulse in rat lung alveolar type II cells: HCO_3^--dependent NH_3 excretion from lung? Pfügers Arch 2007;455:223-239
28 Neesen J, Kirschner R, Ochs M, Schmiedl A, Habermann B, Mueller C, Holstein AF, Nuesslein T, Adham I, Engel W: Disruption of an inner arm dynein heavy chain gene results in asthenozoospermia and reduced ciliary beat frequency. Hum Mol Genet 2001;10:1117-1128.
29 Kultgen PL, Byrd SK, Ostrowski LE, Milgram SL: Characterization of an A-kinase anchoring protein in human ciliary axonemes. Mol Biol Cell 2002;13:4156-4166.
30 Stout SL, Wyatt TA, Adams JJ, Sisson JH: Nitric oxide-dependent cilia regulatory enzyme localization in bovine bronchial epithelial cells. J Histochem Cytochem 2007;55:433-442.
31 Christensen ST, Guerra C, Wada Y, Valentin T, Angeletti RH, Satir P, Hamasaki T: A regulatory light chain of ciliary outer arm dynein in *Tetrahymena thermophila*. J Biol Chem 2001;276:20048-50054.
32 Chilcote TJ, Johnson KA: Phosphorylation of *Tetrahymena* 22S dynein. J Biol Chem1990;265:17257-17266.
33 Gaillard AR, Diener DR, Rosenbaum JL, Sale WS: Flagellar radial spoke protein 3 is an A-kinase anchoring protein (AKAP). J Cell Biol 2001;153:443-448.
34 Gaillard AR, Fox LA, Rhea JM, Craige B, Sale WS: Disruption of the A-kinase anchoring domain in flagellar radial spoke protein 3 results in unregulated axonemal cAMP-dependent protein kinase activity and abnormal flagellar motility. Mol Biol Cell 2006;17:2626-2635.
35 Habermacher G, Sale WS: Regulation of flagellar dynein by phosphorylation of a 138-kD inner arm dynein intermediate chain. J Cell Biol 1997;136:167-176.
36 Kikushima K: Central pair apparatus enhances outer-arm dynein activities through regulation of inner-arm dynein. Cell Motil Cytoskeleton 2009;66:272-280.
37 Sleigh MA, Blake JR, Liron N: The propulsion of mucus by cilia. Am Rev Respir Dis 1988;137:726-741.